A Letters Journal Exploring the Frontiers of Physics

April 2009

EPL, **86** (2009) 28002
doi: 10.1209/0295-5075/86/28002

www.epljournal.org

Crystalline multilayers of the confined Yukawa system

E. C. Oğuz, R. Messina[a] and H. Löwen

Institut für Theoretische Physik II: Weiche Materie, Heinrich-Heine-Universität Düsseldorf Universitätsstraße 1, D-40225 Düsseldorf, Germany

received 9 January 2009; accepted in final form 19 March 2009
published online 29 April 2009

PACS 82.70.Dd – Colloids
PACS 64.70.K- – Solid-solid transitions

Abstract – The phase diagram of Yukawa particles confined between two parallel hard walls is calculated at zero temperature beyond the bilayer regime by lattice-sum-minimization. Tuning the screening, a rich phase behavior is found in the regime bounded by stable two triangular layers and three square layers. In this regime, alternating prism phases with square and triangular basis, structures derived from a hcp bulk lattice, and a structure with two outer layers and two inner staggered rectangular layers, reminiscent of a Belgian waffle iron, are stable. These structures are verifiable in experiments on charged colloidal suspensions and dusty plasma sheets.

If a system is confined to a thin slit geometry, its properties are drastically altered with respect to the bulk [1,2]. In particular, the freezing transition in confined geometry occurs into multilayered crystals whose structure is dictated by an interplay of the interparticle interaction and the confining potential [3–5]. For *hard spheres* between two parallel hard plates of finite separation D, different solid lattices are getting stable with the following cascade for increasing width D: If D equals the hard-sphere diameter, a crystalline monolayer is stable which possesses a two-dimensional triangular ($\triangle$) lattice symmetry. This layer buckles [6–8] upon increasing h such that a two-layer situation is realized. For higher h, there are stable structures that correspond to two intersecting square lattices ($2\square$) or triangular lattices ($2\triangle$) [9,10] with a two-layer rhombic phase in between [6,10]. Beyond bilayers, the transition from the $2\triangle$ to the $3\square$ (simple quadratic trilayer) phase is mediated by prism phases that are made up of alternating prism-like arrays [11,12]. In experiments on strongly screened colloidal suspensions, however, crystals derived from the hexagonal-closed-packed geometry were found as interpolating structures that correspond to four or more layers [13,14]. Beyond the $3\square$ phase, the structures are even more complicated [12,14–16].

Another situation concerns the confined Wigner crystal of repulsive point charges. This classical Coulomb system has been studied when confined between two plates and a bilayer structure is *always* stable[1] even for high separation distances h [17]. Here, we consider a Yukawa system interpolating between the Coulomb interaction and hard spheres[2]. In this case, there are two possibilities for the rhombic bilayer [18]. Experimental realizations can be thought of as charged colloids [19] or dusty plasma sheets [20].

In this paper we study the multilayering for a Yukawa system confined between two hard walls [21] interpolating between the Coulomb and hard-sphere limit. For low screening, appropriate to dusty plasmas, and an external parabolic potential, multilayering was examined by computer simulation and a simple sheet model by Totsuji and coworkers [22]. Structural details of the multilayers, however, were neglected in this shell model approach. Here, we focus on the range of plate distances between the $2\triangle$ and $3\square$ regime and resolve the fine structure using up to four layers as a possible candidate. Apart from prism phases and structures derived from the hexagonal-closed-packed geometry, we find a stable four-layer crystal with

[a] E-mail: messina@thphy.uni-duesseldorf.de

[1] There is a simple and clear electrostatic argument to explain the exclusive stability of bilayers for charges confined between (charged or uncharged) hard walls. Note that two equally charged walls do *not* generate any electric field within the slit, and consequently do not alter the stable structure obtained at any other surface charge (including neutral walls). Hence, if one considers the special case of two walls corresponding to neutralizing backgrounds, then the ground state structure is always a bilayer.

[2] Note that in our model we have point-like particles. Nevertheless, at infinite screening ($\lambda \to \infty$), by taking an effective hard-core diameter corresponding to the smallest lattice constant, one expects to recover the phase behavior of hard spheres.

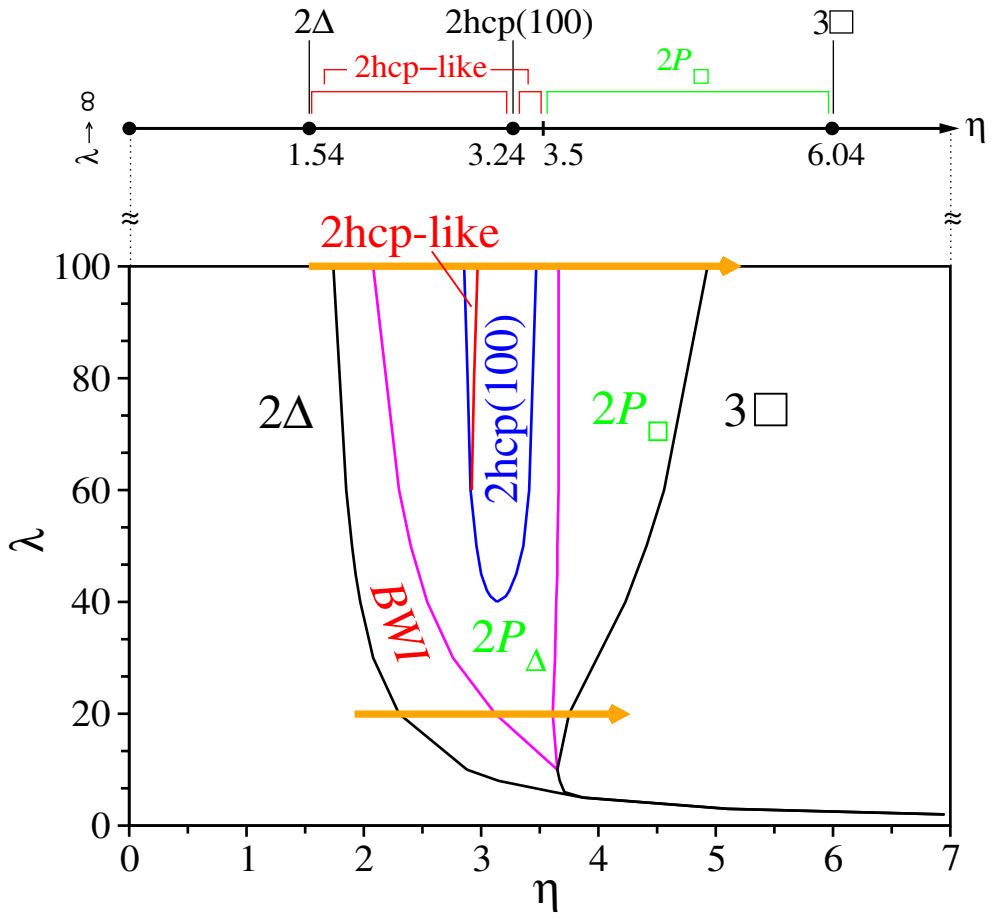

Fig. 1: (Color online) Zero-temperature phase diagram of a Yukawa system confined between two hard plates with screening strength λ and reduced density η, in the multilayer regime between two triangular and three square layers. Stability regions of the Belgian waffle iron (BWI) phase, prism phases with triangular ($2P_{\triangle}$) and square bases ($2P_{\square}$), 2hcp-like and 2hcp(100) phases are shown. For comparison, the hard-sphere limit of infinite screening is shown separately in the top. The arrow indicates a path of constant screening with increasing density.

a structure resembling a Belgian waffle iron (BWI). This BWI structure, which consists of two outer layers and two inner staggered rectangular crystals, does not exist for hard spheres and unscreened charges but is stable in the intermediate screening regime. A control over the achievable crystalline multilayered structures has important applications to the fabrication of nanosieves and filters with desired porosity [23].

In our model, we consider N classical point-like particles interacting *via* the Yukawa pair-potential

$$V(r) = V_0 \frac{\mathrm{e}^{-\kappa r}}{\kappa r}, \tag{1}$$

where r is the interparticle distance, $1/\kappa$ is the screening length, and V_0 denotes an energy amplitude. The particles are confined between two parallel hard plates of area A and separation D which is taken along the z-direction for convenience. At zero temperature, for a given reduced area density $\eta = ND^2/A$, the system will minimize its total potential energy and the resulting optimal structure will be independent on the single energy scale V_0 but will depend on the reduced inverse screening length $\lambda = \kappa D$. By varying this parameter λ, one can interpolate between the unscreened Coulomb limit ($\lambda \to 0$) and the hard-sphere limit ($\lambda \to \infty$) where the interaction is getting very harsh.

For a given screening parameter λ and reduced density η we have performed lattice sum minimizations of a set of candidates. While the stability regimes of mono- and bilayers have been addressed in previous work [18], we focus here on the multilayer regime beyond the stability of the staggered triangular bilayer 2△ phase. This can be achieved by increasing the reduced density η. There is another region at even higher D where the trilayer phase 3□ is stable. Our major goal is to explore the corresponding distance range between the 2△ and 3□ phases and to check for the stability of intervening crystalline multilayers.

As possible candidates for our lattice sum minimization problem, we consider three-dimensional crystals with a two-dimensional periodicity in x- and y-direction whose primitive cell is a parallelogram containing n particles. This parallelogram is spanned by the two lattice vectors

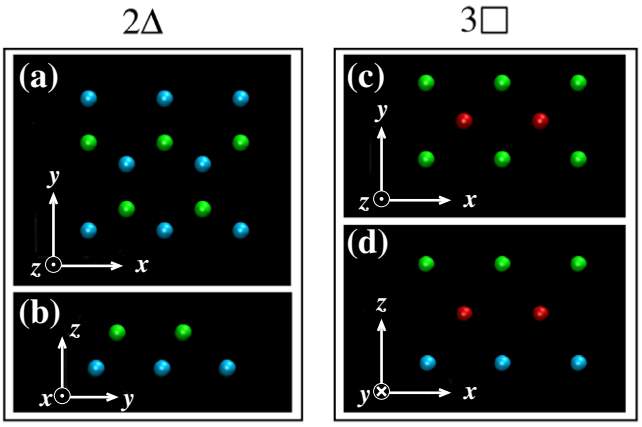

Fig. 2: (Color online) (a) and (b): top view and side view of the 2△ phase. (c) and (d): top view and side view of the 3□ phase. Note that the layer distance does not necessarily coincide with the length of the in-plane square. Particles in different layers are drawn in different colors (green, red, blue).

$\mathbf{a} = a(1,0,0)$ and $\mathbf{b} = a\gamma(\cos\theta, \sin\theta, 0)$, where γ is the aspect ratio ($\gamma = |\mathbf{b}|/|\mathbf{a}| = b/a$), and θ is the angle between $\mathbf{a}$ and $\mathbf{b}$. Furthermore, the n particles are distributed, not necessarily evenly, on m layers in the xy-plane. Hereby we restrict ourselves to layered situations with an up-down inversion symmetry in the averaged occupancy reflecting the up-down symmetry of the confining slit. Under this sole restriction, we consider possible candidates with $n = 2, \ldots, 8$ and $m = 1, \ldots, 4$ up to symmetric four-layer structures with a basis of up to 8 particles. For given η and λ, the total potential energy per particle is minimized with respect to the particle coordinates of the basis and the cell geometry (γ and θ). The resulting stability phase diagram is shown in fig. 1 (see footnote [3]).

First, the boundary of the stability domain of the staggered triangular phase 2△ and the staggered quadratic 3□ are presented, see fig. 1. For convenience, the structure of these two phases are sketched by a top and side view in fig. 2. In between, we observe various stable four-layer structures. For low screening ($\lambda \lesssim 4$), however, there is a direct transition from 2△ to 3□ without any intermediate multilayered crystal consistent with earlier simulations and theoretical results [22]. The $2\triangle \to 3\square$ phase boundary moves to higher densities as the screening λ is lowered so that there are only bilayers for the unscreened Coulomb system ($\lambda \to 0$), see fig. 1 (see footnote [4]).

We now discuss the more complicated intermediate structures of fig. 1. At finite $\lambda \gtrsim 4$, the 2△ transforms discontinuously into a tetra-layered structure ($m = 4$) with $n = 8$. This novel structure shown in fig. 3 is

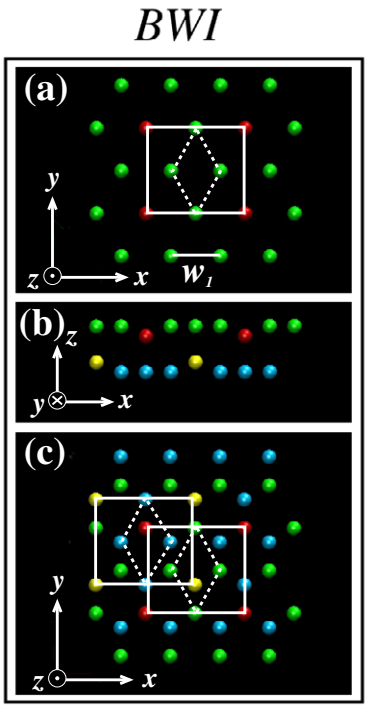

Fig. 3: (Color online) Different views of the Belgian waffle iron (BWI) structure: (a) top view of an outer layer and the next inner layer. The latter corresponds to a rectangular lattice (red particles) with a rhombic decoration (green particles). (b) Side view of all four layers. (c) Top view of all four layers. The width w_1 of the rhombus is shown in (a).

characterized by two inner staggered rectangular lattices (see the red and yellow spheres in fig. 3) and two outer layers with rhombic stripes which are centered relative to the inner rectangular lattice. In principle, this structure can be obtained by a continuous transformation of the 2△ phase. In analogy to Belgian waffles which possess an internal rectangular structure, we call this double staggered situation a "Belgian waffle iron" (BWI) structure, as the corresponding iron mimics the outermost structure qualitatively[5]. The rhombus in the outermost layers is almost symmetric, *i.e.*, the corresponding anisotropy as characterized by the ratio of width w_1 (see fig. 3) and side length of the rhombic is close to 1 (within 1 percent) and only slowly grows with increasing density η.

Next, prism phases with a triangular basis shape $2P_\triangle$ and a square basis shape $2P_\square$ each with $n = 6$ and $m = 4$ (see fig. 4), are stable. In detail, these phases consist of alternating double-layered prism-like arrays with a triangular or square basis structure (see fig. 4). Within the stability regime of prism phases the distances w_2 and w_3 indicated in fig. 4 change about few percents such that with increasing η one can notice a slight decrease of these distances.

[3] One can calculate density jumps [24–26] between the different phases. These turn out to be very small except close to the lower ends of phase stability, *e.g.*, at $\lambda = 10$, $\eta = 3.6$ for the $2P_\square$, and are not shown in fig. 1 for clarity.

[4] As a side remark, we found that a triangular (projected) bilayer, proposed as a stable structure for very small η in [17], is always energetically beaten by a buckled bilayered phase.

[5] We remark that the BWI structure can also be thought of arising from a buckled layer adjacent to a structured layer.

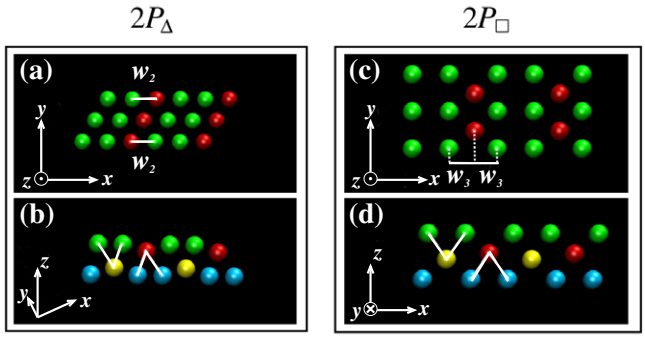

Fig. 4: (Color online) Different views of the prism phases with triangular and quadratic shaped basis: (a) top view of an outer layer and the next inner layer with the appropriate width w_2 and (b) perspective side view of $2P_\triangle$. (c) Top view of an outer layer and the next inner layer with the appropriate width w_3 and (d) side view of $2P_\square$. The alternating prism like arrays are indicated with white lines in (b) and (d).

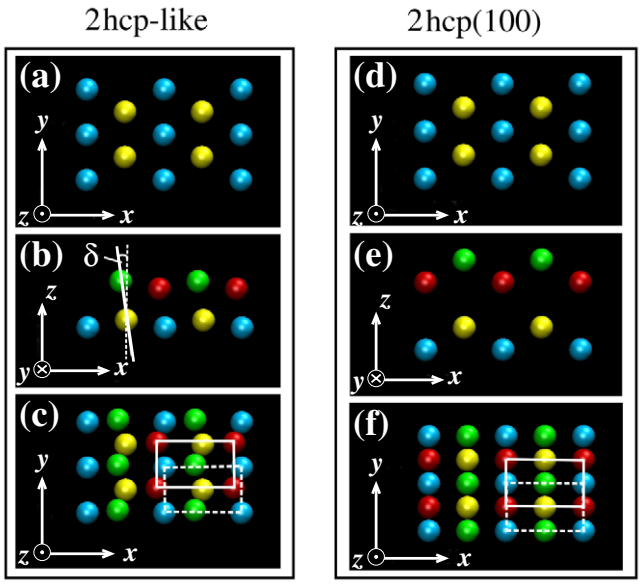

Fig. 5: (Color online) Top views (a), (c), and side view (b) of 2hcp-like as well as top views (d), (f), and side view (e) of 2hcp(100). For $\delta \to 0$, one recovers 2hcp(100). The angle δ results from the additional shift in x-direction of the rectangular bilayers and is shown in (b).

Finally, there are tetralayered structures derivable from the hcp lattice as discussed recently in refs. [13,14], which we accordingly call 2hcp-like and 2hcp(100) phases (see fig. 5). The (100)-plane of the hexagonal-closed-package, possessing a rectangular-shaped basis as sketched in fig. 5, can be thought of as two double-layered rectangular arrays that lie on the top of each other but shifted to each other in the y-direction. The rectangular bilayers of the 2hcp-like structure, on the other hand, experience a further shift in x-direction, resulting in an angle δ (see fig. 5).

For increasing screening constant λ, the topology of the phase diagram reveals the following cascades interpolating between $2\triangle \to 3\square$:

$$\begin{aligned}
&2\triangle \to 3\square,\\
&2\triangle \to \mathrm{BWI} \to 3\square,\\
&2\triangle \to \mathrm{BWI} \to 2P_\triangle \to 2P_\square \to 3\square,\\
&2\triangle \to \mathrm{BWI} \to 2P_\triangle \to \mathrm{2hcp(100)} \to 2P_\triangle \to 2P_\square \to 3\square
\end{aligned} \tag{2}$$

with a remarkable reentrance of the $2P_\triangle$ and finally

$$\begin{aligned}
2\triangle \to \mathrm{BWI} \to 2P_\triangle \to \mathrm{2hcp\text{-}like} \to \mathrm{2hcp(100)}\\
\to 2P_\triangle \to 2P_\square \to 3\square.
\end{aligned} \tag{3}$$

The hard-sphere limit involves the cascade

$$2\triangle \to \mathrm{2hcp\text{-}like} \to \mathrm{2hcp(100)} \to \mathrm{2hcp\text{-}like} \to 2P_\square \to 3\square,$$

which is qualitatively different from those at finite screening as the BWI and the $2P_\triangle$ are missing. Therefore, even at high $\lambda \approx 100$ there are considerable deviations from the ultimate hard-sphere limit.

All transitions involved here for finite λ are of first order except the 2hcp-like $\to$ 2hcp(100) one which is continuous. This is illustrated in fig. 6 where the distance Δd between the outermost and the next inner layer is shown along the arrows indicated in fig. 1, *i.e.*, for increasing density η at fixed screening $\lambda = 20$ and $\lambda = 100$ leading to the full

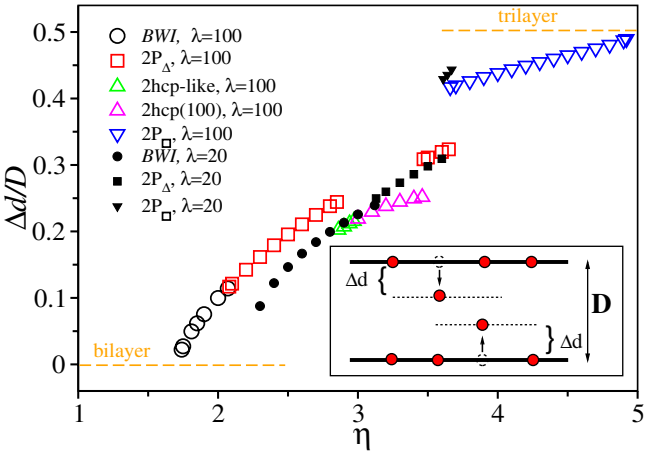

Fig. 6: (Color online) Reduced distance $\Delta d/D$ between the outermost and the next inner layer as a function of density η for fixed $\lambda = 20$ and $\lambda = 100$. The limits of a trilayer and bilayer situations are indicated by the dashed lines. The geometric meaning of Δd, developing of the distance between inner and outer layers is shown in the inset.

transition cascade (see (3)). The geometric meaning of Δd is sketched in the inset of fig. 6. The reduced quantity $\Delta d/D$ can serve as an order parameter for multilayering in the sense that $\Delta d/D = 0.5$ for centered trilayers and (formally) $\Delta d/D = 0$ for symmetric bilayers. Multilayers beyond $m = 3$ are characterized by an intermediate value of $\Delta d/D$. Moreover, for an equilayer-spacing, $\Delta d/D$ is $1/(m-1)$. For $\lambda = 100$, clearly, the transition from $2\triangle$ to BWI is accompanied with a jump from zero to $\Delta d/D = 0.0221$ ($\Delta d/D = 0.0933$ for $\lambda = 20$) implying a

first-order transition although a second-order transition would have been not precluded by lattice symmetry. The subsequent BWI $\to 2P_\triangle$ transition is discontinuous (though the jump in $\Delta d/D$ is tiny in fig. 6) while the 2hcp-like $\to$ 2hcp(100) transition is continuous. The latter transition occurs as the angle δ approaches zero as indicated in fig. 5. For $\lambda = 20$, there are only discontinuous transitions along the cascade (2). In the limit of hard spheres, volume fraction calculations among the considered candidates show that the transitions $2\triangle \to$ 2hcp-like $\to$ 2hcp(100) $\to$ 2hcp-like are of second order, while the transition 2hcp-like $\to 2P_\square$ is of first order. The transition $2P_\square \to 3\square$ occurs in the hard-sphere limit continuously, as opposed to finite λ.

To summarize, we investigated the stability phase diagram of a confined classical one-component Yukawa system in the transition regime $2\triangle \to 3\square$. Various crystalline tetra-layer structures are intervening including a novel one with a BWI, phases of alternating prisms $2P_\triangle$, $2P_\square$, and structures derived from a bulk hcp structure (2hcp-like and 2hcp(100)). For the unscreened Coulomb system only bilayers are stable while in the opposite (hard-sphere) limit the sequence for increasing density is $2\triangle \to$ 2hcp-like $\to$ 2hcp(100) $\to$ 2hcp-like $\to$ $2P_\square \to 3\square$ [13]. Our theoretical results are verifiable in experiments on colloidal suspensions. In fact, all phases were found in recent experimental investigations except the BWI structure which, however, resembles experimentally determined superstructures [19]. Furthermore, strongly interacting dust particles in plasmas are typically in the intermediate screening regime at low reduced temperatures and are, therefore, other candidates for an experimental system where the multilayer phases proposed here are, in principle, observable.

Future work should focus on the inclusion of higher layer numbers m. We have examined the special case with $m = 6$ layers which was called pre-3$\square$ in ref. [13]. This structure, however, was not found to be stable in the range of λ considered in this work. Next, charged walls will lead to a soft exponentially screened wall-particle interaction [27] rather than a hard wall which would introduce more parameters in the corresponding model [22]. In this situation, the multilayering scenario is expected to favor phases that have more weight in the inner layers. The effect of finite temperature [28] needs more investigation; temperature can be viewed as an additional coordinate in the two-dimensional phase diagram presented in fig. 1. We expect, however, no drastic change in the phase diagram topology. Finally, we remark that genetic minimization algorithms [29] might be a versatile tool to explore even more complicated crystalline layer structures.

* * *

We thank T. Palberg, H. J. Schöpe, A. Wynveen, and F. Ramiro-Manzano for helpful discussions. This work was supported by the DFG (SFB TR6, project D1).

REFERENCES

[1] Dietrich S. and Haase A., *Phys. Rep.*, **260** (1995) 1.
[2] Drake J. M. and Klafter J., *Phys. Today*, **43**, issue No. 5 (1990) 46.
[3] Zangi R. and Rice S., *Phys. Rev. E*, **61** (2000) 660.
[4] Ayappa K. G. and Ghatak C., *J. Chem. Phys.*, **117** (2002) 5373.
[5] Cornelissens Y. G., Partoens B. and Peeters F. M., *Physica E*, **8** (2000) 314.
[6] Schmidt M. and Löwen H., *Phys. Rev. Lett.*, **76** (1996) 4552.
[7] Chou T. and Nelson D. R., *Phys. Rev. E*, **48** (1993) 4611.
[8] Radzihovsky L., Frey E. and Nelson D. R., *Phys. Rev. E*, **63** (2001) 031503.
[9] Pieranski P., Strzlecki L. and Pansu B., *Phys. Rev. Lett.*, **50** (1983) 900.
[10] Schmidt M. and Löwen H., *Phys. Rev. E*, **55** (1997) 7228.
[11] Neser S., Bechinger C., Leiderer P. and Palberg T., *Phys. Rev. Lett.*, **79** (1997) 2348.
[12] Fortini A. and Dijkstra M., *J. Phys.: Condens. Matter*, **18** (2006) L371.
[13] Ramiro-Manzano F., Bonet E., Rodriguez I. and Meseguer F., *Phys. Rev. E*, **76** (2007) 050401.
[14] Barreira Fontecha A., Palberg T. and Schöpe H. J., *Phys. Rev. E*, **76** (2007) 050402.
[15] Ramiro-Manzano F., Meseguer F., Bonet E. and Rodriguez I., *Phys. Rev. Lett.*, **97** (2006) 028304.
[16] Schöpe H. J., Barreira Fontecha A., König H., Marques Hueso J. and Biehl R., *Langmuir*, **22** (2006) 1828.
[17] Goldoni G. and Peeters F. M., *Phys. Rev. B*, **53** (1995) 4591.
[18] Messina R. and Löwen H., *Phys. Rev. Lett.*, **91** (2003) 146101.
[19] Barreira Fontecha A. and Schöpe H. J., *Phys. Rev. E*, **77** (2008) 061401.
[20] Morfill G. E., Ivlev A. V., Rubin-Zuzic M., Knapek C. A., Pompl R., Antonova T. and Thomas H. M., *Appl. Phys. B: Lasers Opt.*, **89** (2007) 527.
[21] For a recent study of the fluid phase, see: Klapp S. H. L., Zeng Y., Qu D. and von Klitzing R., *Phys. Rev. Lett.*, **100** (2008) 118303.
[22] Totsuji H., Kishimoto T. and Totsuji C., *Phys. Rev. Lett.*, **78** (1996) 3113.
[23] Tierno P., Thonke K. and Goedel W. A., *Langmuir*, **21** (2005) 9476.
[24] Graf H. and Löwen H., *Phys. Rev. E*, **57** (1998) 5744.
[25] Van Roij R., Dijkstra M. and Hansen J. P., *Phys. Rev. E*, **59** (1999) 2010.
[26] Warren P. B., *J. Chem. Phys.*, **112** (2000) 4683.
[27] Löwen H., Härtel A., Barreira Fontecha A., Schöpe H. J., Allahyarov E. and Palberg T., *J. Phys.: Condens. Matter*, **20** (2008) 404221.
[28] Messina R. and Löwen H., *Phys. Rev. E*, **73** (2006) 011405.
[29] Gottwald D., Likos C. N., Kahl G. and Löwen H., *J. Chem. Phys.*, **122** (2005) 074903.